The general theory of first-order spatio-temporal distortions of Gaussian pulses and beams

Selcuk Akturk, Xun Gu, Pablo Gabolde and Rick Trebino

School of Physics, Georgia Institute of Technology, Atlanta, Georgia 30332-0430, USA
akturk@socrates.physics.gatech.edu

Abstract: We present a rigorous, but mathematically relatively simple and elegant, theory of first-order spatio-temporal distortions, that is, couplings between spatial (or spatial-frequency) and temporal (or frequency) coordinates, of Gaussian pulses and beams. These distortions include pulse-front tilt, spatial dispersion, angular dispersion, and a less well-known distortion that has been called "time vs. angle." We write pulses in four possible domains, xt, xω, kω, and kt; and we identify the first-order couplings (distortions) in each domain. In addition to the above four "amplitude" couplings, we identify four new spatio-temporal "phase" couplings: "wave-front rotation," "wave-front-tilt dispersion," "angular temporal chirp," and "angular frequency chirp." While there are eight such couplings in all, only two independent couplings exist and are fundamental in each domain, and we derive simple expressions for each distortion in terms of the others. In addition, because the dimensions and magnitudes of these distortions are unintuitive, we provide normalized, dimensionless definitions for them, which range from -1 to 1. Finally, we discuss the definitions of such quantities as pulse length, bandwidth, angular divergence, and spot size in the presence of spatio-temporal distortions. We show that two separate definitions are required in each case, specifically, "local" and "global" quantities, which can differ significantly in the presence of spatio-temporal distortions.

©2005 Optical Society of America

OCIS codes: (320.5550) Pulses; (320.7100) Ultrafast measurements

References and Links

1. S. Akturk, M. Kimmel, P. O'Shea, and R. Trebino, "Measuring spatial chirp in ultrashort pulses using single-shot Frequency-Resolved Optical Gating," Opt. Express **11**, 68-78 (2003).
   http://www.opticsexpress.org/abstract.cfm?URI=OPEX-11-1-68
2. X. Gu, S. Akturk, and R. Trebino, "Spatial chirp in ultrafast optics," Opt. Commun. **242**, 599-604 (2004).
3. S. Akturk, M. Kimmel, P. O'Shea, and R. Trebino, "Measuring pulse-front tilt in ultrashort pulses using GRENOUILLE," Opt. Express **11**, 491-501 (2003).
   http://www.opticsexpress.org/abstract.cfm?URI=OPEX-11-5-491
4. K. Varju, A. P. Kovacs, G. Kurdi, and K. Osvay, "High-precision measurement of angular dispersion in a CPA laser," Appl. Phys. B-Lasers and Optics **B74[Suppl]**, 259-263 (2002).
5. K. Varju, A. P. Kovacs, and K. Osvay, "Angular dispersion of femtosecond pulses in a Gaussian beam," Opt. Lett. **27**(22), 2034-2036 (2002).
6. O. E. Martinez, "Pulse distortions in tilted pulse schemes for ultrashort pulses," Opt. Commun. **59**(3), 229-232 (1986).
7. C. Dorrer, E. M. Kosik, and I. A. Walmsley, "Spatio-temporal characterization of ultrashort optical pulses using two-dimensional shearing interferometry," Appl. Phys. B-Lasers and Optics **74 [suppl.]**, 209-219 (2002).
8. Z. Bor, B. Racz, G. Szabo, M. Hilbert, and H. A. Hazim, "Femtosecond pulse front tilt caused by angular dispersion," Opt. Engineering **32**(10), 2501-2503 (1993).
9. J. Hebling, "Derivation of pulse-front tilt casued by angular dispersion," Opt. Quantum Eng. **28**, 1759-1763 (1996).

10. I. Z. Kozma, G. Almasi, and J. Hebling, "Geometrical optical modeling of femtosecond setups having angular dispersion," Appl. Phys. B-Lasers and Optics B **76**, 257-261 (2003).
11. S. Akturk, X. Gu, E. Zeek, and R. Trebino, "Pulse-front tilt caused by spatial and temporal chirp," Opt. Express **12**, 4399-4410 (2004). http://www.opticsexpress.org/abstract.cfm?URI=OPEX-12-19-4399
12. O. E. Martinez, "Matrix formalism for pulse compressors," IEEE J. Quantum. Electron. **24**, 2530-2536 (1988).
13. O. E. Martinez, "Matrix Formalism for Dispersive Laser Cavities," IEEE J. Quantum. Electron. **25**, 296-300 (1989).
14. S. P. Dijaili, A. Dienes, and J. S. Smith, "ABCD Matrices for dispersive pulse propagation," IEEE J. Quantum. Electron. **26**, 1158-1164 (1990).
15. M. A. Larotonda and A. A. Hnilo, "Short laser pulse parameters in a nonlinear medium: different approximations of the ray-pulse matrix," Opt. Commun. **183**, 207-213 (2000).
16. Q. Lin and S. Wang, "Spatial-temporal coupling in a grating-pair pulse compression system analysed by matrix optics," Opt. Quantum Electron. **27**, 785-798 (1995).
17. A. G. Kostenbauder, "Ray-Pulse Matrices: A Rational Treatment for Dispersive Optical Systems," IEEE J. Quantum. Electron. **26**, 1148-1157 (1990).
18. M. Born and E. Wolf, Principles of Optics: Electromagnetic Theory of Propagation, Interference and Diffraction of Light (Cambridge Univ Pr, 1999).
19. A. E. Siegman, *Lasers* (Univ Science Books, 1986).
20. I. S. Gradshteyn and I. M. Ryzhik, *Table of integrals, series and products* (Academic Press, 1994).
21. K. Osvay, A. Kovacs, Z. Heiner, G. Kurdi, J. Klebniczki, and M. Csatari, "Angular Dispersion and Temporal Change of Femtosecond Pulses From Misaligned Pulse Compressors," IEEE JSTQE **10**(1), 213-220 (2004).
22. O. E. Martinez, "Grating and prism compressors in the case of finite beam size," J. Opt. Soc. Am. B **3**, 929-934 (1986).
23. D. J. Kane and R. Trebino, "Characterization of Arbitrary Femtosecond Pulses Using Frequency Resolved Optical Gating," IEEE J. Quantum Electron. **29**, 571-579 (1993).
24. P. O'Shea, M. Kimmel, X. Gu, and R. Trebino, "Highly simplified device for ultrashort-pulse measurement," Opt. Lett. **26**(12), 932-934 (2001).
25. R. Trebino, *Frequency-Resolved Optical Gating* (Kluwer Academic Publishers, Boston, 2002).
26. P. Gabolde and R. Trebino, "Self-referenced measurement of the complete electric field of ultrashort pulses," Opt. Expr.ess **12**, 4423-4429 (2004).
   http://www.opticsexpress.org/abstract.cfm?URI=OPEX-12-19-4423
27. R. G. Lane and M. Tallon, "Wave-front reconstruction using a Shack-Hartmann sensor," Appl. Opt. **31**, 6902-6908 (1992).

1. Introduction

Ultrashort laser pulses are usually expressed separately in terms of the temporal and spatial dependences of their electric field. In this formalism, it is implicitly assumed that the spatial or spatial frequency dependence of the pulse is completely separable from time or frequency dependence. However, this assumption often fails, as the generation and manipulation of ultrashort pulses require the introduction of couplings between the spatial or spatial-frequency and temporal or frequency coordinates (hereafter referred to as "spatio-temporal couplings" or "spatio-temporal distortions" in this text). Moreover, taking advantage of the spatio-temporal dependences of ultrashort pulses also allows applications, such as pulse compression and shaping, not possible in their absence. For these reasons, spatio-temporal couplings are receiving increased attention from researchers in recent years.

To date, numerous researchers have studied individual spatio-temporal couplings. Spatial chirp (SPC) and its parameterization and measurement were considered in references [1, 2]. The study of angular dispersion (AGD) and its relation to pulse-front tilt (PFT) were also undertaken by several researchers [3-7]. Most of this work, however, has concentrated on a particular coupling or two, rather than explicitly investigating all possible relations between spatio-temporal couplings in different domains (as we will do here).

Indeed, the subject of spatio-temporal distortions is proving to be more subtle than previously thought. These effects are not independent because the pulse fields expressed in different domains are related by Fourier transforms. This fact was exploited to derive a relation between AGD and PFT [6-10], with the result that it is widely believed that AGD and PFT are equivalent phenomena. This observation is, however, not general, and, as only

recently shown in [11], PFT is also generated by simultaneous spatial and temporal chirp. In related work, Gu et al. [2] showed that even defining SPC is not a trivial matter, and two possible, physically distinct, approaches are possible.

All of the subtleties encountered in the past and the broad range of possible applications suggest that ultrafast optics researchers would benefit extensively from a detailed study of spatio-temporal couplings. Such a study would also provide a much more intuitive understanding of the behavior of ultrashort pulses.

In this publication, we present a general theory of spatio-temporal couplings. Specifically, we investigate all possible coupling effects in the various domains, and we derive analytical expressions that, not only properly describe them, but also yield explicit relations between different effects. We consider beams that are Gaussian in the transverse spatial (x) domain and hence also in its Fourier conjugate domain (k). We also consider pulses that are Gaussian in time (t) and hence also in frequency (ω).

Previously identified spatio-temporal couplings include pulse-front tilt (in the x-t domain), spatial dispersion (in the x-ω domain), angular dispersion (in the k-ω domain) and a less well-known distortion called "time vs. angle" (in the k-t domain). These distortions occur in the real component of the coupling and hence can be called amplitude couplings. Here we identify four new spatio-temporal distortions, which occur in the *imaginary* part of the coupling in the relevant domains and hence are spatio-temporal *phase* distortions. They are "wave-front rotation" (in the x-t domain), "wave-front-tilt dispersion" (in the x-ω domain), "angular frequency chirp" (in the k-ω domain), and "angular temporal chirp" (in the k-t domain). While there are eight spatio-temporal distortions in all (one real and one imaginary for each of the four domains), only two independent distortions exist overall. Once the amplitude and phase couplings are determined in a given domain, the analogous couplings are determined in each of the other three domains by simple Fourier transformation. Our approach is simply to write Gaussian ultrashort pulses in the four possible domains, identify the first-order (i.e. lowest order) couplings in each domain, and derive explicit relations between various couplings. Each spatio-temporal distortion can then be written as the weighted sum of two distortions in a neighboring domain.

2. The approach

Our approach is motivated by an established matrix formalism. Different matrix methods for propagating Gaussian ultrashort pulses with Gaussian spatial profiles with spatio-temporal couplings have been demonstrated previously [12-16]. The most comprehensive approach was given by Kostenbauder [17], who used 4×4 "ray-pulse matrices" to model optical elements and their effects in transforming input pulse parameters (expressed as a vector) to output ones. The finite beam size, wave-front radius of curvature, pulse length, and chirp can be taken into account [17] (see the appendix of reference [11], for example). Two spatio-temporal distortion parameters are also included, which involve both real and imaginary couplings. This involves expressing the electric field of the pulse in the form:

$$
E(x,t) = \exp\left\{ -i\frac{\pi}{\lambda_0} \begin{pmatrix} x \\ -t \end{pmatrix}^T Q^{-1} \begin{pmatrix} x \\ t \end{pmatrix} \right\} =
$$

$$
\exp\left[-i\frac{\pi}{\lambda_0} \left(\left(Q^{-1}\right)_{11} x^2 + \left(Q^{-1}\right)_{12} xt - \left(Q^{-1}\right)_{21} xt - \left(Q^{-1}\right)_{22} t^2 \right) \right]
$$

(1)

where $\left(Q^{-1}\right)_{12} = -\left(Q^{-1}\right)_{21}$, so we will combine these two quantities in all future results.

The ray-pulse matrix for an optical system that introduces couplings up to the first order can be written as:

$$K = \begin{vmatrix} \dfrac{\partial x_{out}}{\partial x_{in}} & \dfrac{\partial x_{out}}{\partial \theta_{in}} & 0 & \dfrac{\partial x_{out}}{\partial v_{in}} \\[2mm] \dfrac{\partial \theta_{out}}{\partial x_{in}} & \dfrac{\partial \theta_{out}}{\partial \theta_{in}} & 0 & \dfrac{\partial \theta_{out}}{\partial v_{in}} \\[2mm] \dfrac{\partial t_{out}}{\partial x_{in}} & \dfrac{\partial t_{out}}{\partial \theta_{in}} & 1 & \dfrac{\partial t_{out}}{\partial v_{in}} \\[2mm] 0 & 0 & 0 & 1 \end{vmatrix} = \begin{bmatrix} A & B & 0 & E \\ C & D & 0 & F \\ G & H & 1 & I \\ 0 & 0 & 0 & 1 \end{bmatrix} \tag{2}$$

Then, the field at the output of the element is found by the propagation expression:

$$Q_{out} = \left\{ \begin{bmatrix} A & 0 \\ G & 1 \end{bmatrix} Q_{in} + \begin{bmatrix} B & E/\lambda_0 \\ H & I/\lambda_0 \end{bmatrix} \right\} \cdot \left\{ \begin{bmatrix} C & 0 \\ 0 & 0 \end{bmatrix} Q_{in} + \begin{bmatrix} D & F/\lambda_0 \\ 0 & 1 \end{bmatrix} \right\}^{-1} \tag{3}$$

Equation (1) can be written in a more compact manner by absorbing the constant and inverses in the tilde symbol, and substituting the indices with coordinates:

$$E(x,t) \propto \exp\left\{ \tilde{Q}_{xx}x^2 + 2\tilde{Q}_{xt}xt - \tilde{Q}_{tt}t^2 \right\} \tag{4}$$

so that,

$$Q_{in} = \begin{bmatrix} Q_{11} & Q_{12} \\ -Q_{12} & Q_{22} \end{bmatrix} = i\frac{\lambda_0}{\pi} \begin{bmatrix} \tilde{Q}_{xx} & \tilde{Q}_{xt} \\ -\tilde{Q}_{xt} & \tilde{Q}_{tt} \end{bmatrix}^{-1} \tag{5}$$

The diagonal elements of $\tilde{Q}$ are:

$$\tilde{Q}_{xx} = -i\frac{\pi}{\lambda_0 R(z)} - \frac{1}{w^2(z)} \tag{6}$$

$$\tilde{Q}_{tt} = -i\beta + \frac{1}{\tau^2} \tag{7}$$

where λ is the pulse center wavelength, R is the beam radius of curvature, w is the spot size, β is temporal chirp and τ is temporal pulse width. The off-diagonal Q_{xt} term gives the coupling between space and time and will be examined in detail later in the next section. Procedure for obtaining explicit mathematical expression for this coupling term will be given in section 5. The matrix formed by the Q coefficients can be propagated easily through an optical element using matrices given in [17].

The question is how to obtain all the various possible spatio-temporal distortions from the Q matrix. And what spatio-temporal distortions are possible anyway? Our approach throughout this publication will be as follows: we will start with the expression in Eq. (4). In this expression, Gaussian spatial and temporal profiles are assumed. Equation (4) inherently

contains the full space-time pulse information (up to second order). We will then simply calculate the electric field in other domains, namely, the (x,ω), (k,ω) and (k,t) domains by performing (inverse) Fourier transforms. In each domain we will identify coefficients like the Q s in the (x,t) domain. The cross terms in each domain will be the spatio-temporal couplings in that particular domain. This will determine essentially all of the possible first-order couplings as well as the relations between them.

We concentrate on only one transverse spatial coordinate, the transverse 'x', as generalization to both transverse coordinates (x and y) is trivial. Also, one could easily generalize our formalism to an arbitrary spatial and/or temporal profile by using computational methods. Propagating more general fields can be accomplished using Fresnel-Kirchoff integrals [18, 19].

3. The pulse electric field expressions in different domains

Our starting point is Eq. (4):

$$E(x,t) \propto \exp\left\{ \widetilde{Q}_{xx}x^2 + 2\widetilde{Q}_{xt}xt - \widetilde{Q}_{tt}t^2 \right\}$$

The $\tilde{Q}$ coefficients here are complex. The physical meanings of these coefficients are as follows:

$$\mathrm{Re}\left\{\tilde{Q}_{xx}\right\} \leftrightarrow \text{beam spot size (BSS)}$$
$$\mathrm{Im}\left\{\tilde{Q}_{xx}\right\} \leftrightarrow \text{wave-front curvature (WFC)}$$
$$\mathrm{Re}\left\{\tilde{Q}_{tt}\right\} \leftrightarrow \text{temporal pulse width (TPW)}$$
$$\mathrm{Im}\left\{\tilde{Q}_{tt}\right\} \leftrightarrow \text{temporal chirp (TCH)}$$

(8)

where we use a double-headed arrow, rather than an equals sign, because, while the parameters are equivalent, they are not equal: various constants are also involved, as well as inverse and/or square root operations (see Eq.(6) and (7)). For example, the temporal pulse width is proportional to the inverse square root of $\mathrm{Re}\left\{Q_{tt}\right\}$.

The physical meanings of the real and imaginary parts of the complex coupling term $\tilde{Q}_{xt}$ can be seen from the following. Because the pulse intensity profile is given by the squared magnitude of the E-field, the real part of Q_{xt} yields a position-time coupling in the intensity profile vs. x and t. This effect is clearly the renowned pulse-front tilt (PFT). In its presence, the arrival time of maximum intensity will vary across the transverse direction.

The imaginary part of Q_{xt}, on the other hand, yields a quantity not previously considered, to our knowledge. Specifically, it yields a time-and-position-dependent *phase*. Physically, this phase distortion causes the wave-front of the pulse to *rotate in time*, so we refer to it as "wave-front rotation" (WFR). This phenomenon is illustrated in the movie below (see figure 1). As a result, we write:

$$\mathrm{Re}\left\{\tilde{Q}_{xt}\right\} \leftrightarrow \text{pulse-front tilt (PFT)}$$
$$\mathrm{Im}\left\{\tilde{Q}_{xt}\right\} \leftrightarrow \text{wave-front rotation (WFR)}$$
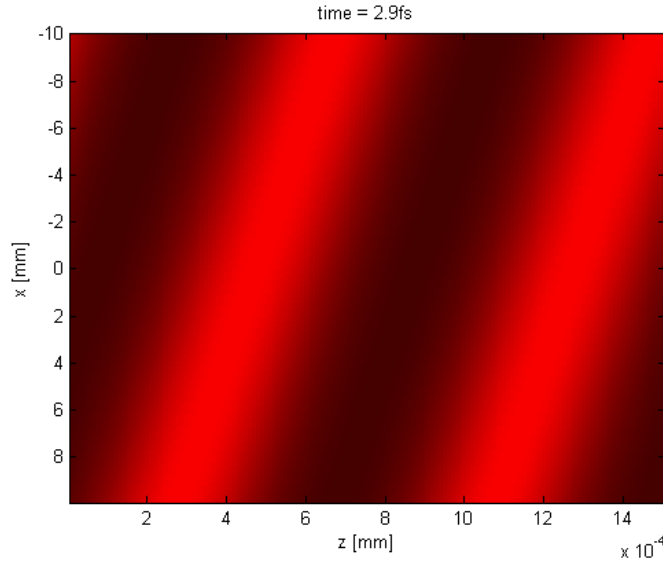
(9)

Fig. 1. The effect of the WFR. The movie shows the wave fronts in (x,t) domain as a function of time and position (file size 2.26 MB).

The field can now be Fourier transformed to the (x,ω) domain:

$$E(x,\omega) = \frac{1}{2\pi} \int E(x,t)e^{-i\omega t}\,dt \qquad (10)$$

This integral, and all of the additional integrals that we will encounter, are of the same simple closed form [20]:

$$\int_{-\infty}^{\infty} \exp\left(-p^2 x^2 \pm qx\right)dx = \exp\left(\frac{q^2}{4p}\right)\frac{\sqrt{\pi}}{|p|} \qquad (11)$$

We will also omit constant factors in front of the field expressions as they do not carry any significance for our purposes. After carrying out the integral in Eq. (10), we find the field in (x,ω) domain to be:

$$E(x,\omega) \propto \exp\left\{ R_{xx}x^2 + 2R_{x\omega}x\omega - R_{\omega\omega}\omega^2 \right\} \qquad (12)$$

where the new set of coefficients, the 'R's, can be expressed in terms of the $\tilde{Q}$'s:

$$R_{xx} = \widetilde{Q}_{xx} + \frac{\widetilde{Q}_{xt}^2}{\widetilde{Q}_{tt}}$$

$$R_{x\omega} = \frac{-i}{2} \frac{\widetilde{Q}_{xt}}{\widetilde{Q}_{tt}} \qquad\qquad (13)$$

$$R_{\omega\omega} = \frac{1}{4\widetilde{Q}_{tt}}$$

Following the same arguments that we used for the (x,t) domain, these coefficients can be identified in terms of their physical meanings:

$$\mathrm{Re}\{R_{xx}\} \leftrightarrow \text{ beam spot size (BSS)}$$

$$\mathrm{Im}\{R_{xx}\} \leftrightarrow \text{ wave-front curvature (WFC)}$$

$$\mathrm{Re}\{R_{\omega\omega}\} \leftrightarrow \text{ bandwidth (BDW)}$$

$$\mathrm{Im}\{R_{\omega\omega}\} \leftrightarrow \text{ frequency chirp (FCH)} \qquad\qquad (14)$$

$$\mathrm{Re}\{R_{x\omega}\} \leftrightarrow \text{ spatial chirp (SPC)}$$

$$\mathrm{Im}\{R_{x\omega}\} \leftrightarrow \text{ wave-front-tilt dispersion (WFD)}$$

Note that, in the (x,ω) domain, we have distinguished the "frequency chirp" (FCH) from the "temporal chirp" (TCH) in the (x,t) domain. Although the temporal chirp and frequency chirp are essentially equivalent for Gaussian pulses, conversion from one to the other also requires the pulse length or bandwidth, so we have distinguished them here to emphasize their different domains. This will also allow us to extend these results to higher orders for more complex pulses, for which this equivalence no longer holds.

The real part of the coupling term, $R_{x\omega}$, yields the well-known spatial chirp. The effect of the imaginary part of $R_{x\omega}$ has not been considered previously. It causes the wave-front to be tilted by an amount that depends on the frequency, as displayed in the movie below, hence our name for this quantity: "wave-front-tilt dispersion" (WFD).

At this point, we can begin to see relations between various spatio-temporal distortions. Eq. (13) yields an explicit formula that relates PFT and SPC. We will discuss it in the next section.

Next, we inverse-Fourier-transform Eq. (12) to the (k,ω) domain and obtain:

$$E(k,\omega) \propto \exp\left\{S_{kk}k^2 + 2S_{k\omega}k\omega - S_{\omega\omega}\omega^2\right\} \qquad\qquad (15)$$

The coefficients 'S' are related to R as:

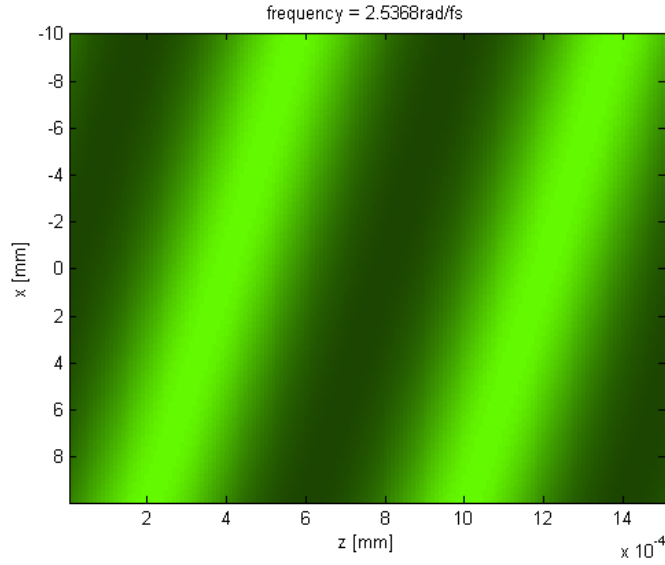Fig. 2. The effect of the WFD. The movie shows the wave fronts in (x,ω) as a function of frequency and position (file size 2.06 MB).

$$S_{kk} = \frac{1}{4R_{xx}}$$

$$S_{k\omega} = \frac{i}{2}\frac{R_{x\omega}}{R_{xx}} \tag{16}$$

$$S_{\omega\omega} = R_{\omega\omega} + \frac{R_{x\omega}^2}{R_{xx}}$$

A more elegant expression can be obtained if we relate the 2x2 matrix formed by the S coefficients to the one formed by Q coefficients, namely:

$$\left[\tilde{Q}\right] = \begin{bmatrix} \tilde{Q}_{xx} & \tilde{Q}_{xt} \\ -\tilde{Q}_{xt} & \tilde{Q}_{tt} \end{bmatrix} \tag{17}$$

$$\left[S\right] = \begin{bmatrix} S_{kk} & S_{k\omega} \\ -S_{k\omega} & S_{\omega\omega} \end{bmatrix} \tag{18}$$

Then, it is easy to show that:

$$\left[S\right] = \frac{1}{4}\left[\tilde{Q}^T\right]^{-1} \tag{19}$$

Where the superscript T indicates non-conjugate matrix transpose.

Now we identify the S coefficients:

$$\text{Re}\{S_{kk}\} \leftrightarrow \text{ angular divergence (ADV)}$$

$$\text{Im}\{S_{kk}\} \leftrightarrow \text{ angular phase-front curvature (APC)}$$

$$\text{Re}\{S_{\omega\omega}\} \leftrightarrow \text{ bandwidth (BDW)}$$

$$\text{Im}\{S_{\omega\omega}\} \leftrightarrow \text{ frequency chirp (FCH)}$$ (20)

$$\text{Re}\{S_{k\omega}\} \leftrightarrow \text{ angular dispersion (AGD)}$$

$$\text{Im}\{S_{k\omega}\} \leftrightarrow \text{ angular spectral chirp (ASC)}$$

where the diagonal parameter, $\text{Im}\{S_{kk}\}$, is related to the wave-front curvature in the space (x) domain. But, in the spatial-frequency (k) domain, we refer to it as the "angular phase-front curvature" (APC) to more accurately reflect its effect on the beam. This distinction is analogous to the distinction we have made between the temporal and frequency chirp, both of which have relationships that depend on other parameters and which become more complex when the dependence is non-Gaussian. The real off-diagonal parameter, $\text{Re}\{S_{k\omega}\}$, is the angular dispersion (AGD). Physically, it yields the angle between the propagation directions of different frequency components. Note that, in general, it is different from the angle between phase fronts of different frequencies, as explained in [21]. The imaginary part, $\text{Im}\{S_{k\omega}\}$, is a new quantity, and it indicates the presence of what we will call "angular spectral chirp" (ASC) because it involves a variation of the frequency with angle. Its effect is analogous to the one shown in figure 2, but the y-axis represents the k-vector instead of position.

Finally, we inverse Fourier-transform Eq. (15) to the (k,t) domain:

$$E(k,t) \propto \exp\{P_{kk}k^2 + 2P_{kt}kt - P_{tt}t^2\}$$ (21)

The 'P' coefficients are related to the S coefficients as:

$$P_{kk} = S_{kk} + \frac{S_{k\omega}^2}{S_{\omega\omega}}$$

$$P_{kt} = \frac{i}{2}\frac{S_{k\omega}}{S_{\omega\omega}}$$ (22)

$$P_{tt} = \frac{1}{4S_{\omega\omega}}$$

Just as S and Q are matrix-inverses, we can also write the P-matrix as the inverse of the R matrix:

$$[P] = \frac{1}{4}[R^T]^{-1}$$ (23)

where:

$$[R] = \begin{bmatrix} R_{xx} & R_{x\omega} \\ -R_{x\omega} & R_{\omega\omega} \end{bmatrix} \qquad [P] = \begin{bmatrix} P_{kk} & P_{kt} \\ -P_{kt} & P_{tt} \end{bmatrix}$$ (24)

The superscript T indicates a non-conjugate matrix transpose.

The *P* coefficients can be identified as:

$$\text{Re}\{P_{kk}\} \leftrightarrow \text{ angular divergence (ADV)}$$
$$\text{Im}\{P_{kk}\} \leftrightarrow \text{ angular phase-front curvature (APC)}$$
$$\text{Re}\{P_{tt}\} \leftrightarrow \text{ temporal pulse width (TPW)}$$
$$\text{Im}\{P_{tt}\} \leftrightarrow \text{ temporal chirp (TCH)}$$
$$\text{Re}\{P_{kt}\} \leftrightarrow \text{ time vs. angle (TVA)}$$
$$\text{Im}\{P_{kt}\} \leftrightarrow \text{ angular temporal chirp (ATC)}$$

(25)

The real off-diagonal parameter here, $\text{Re}\{P_{kt}\}$, is the pulse "time vs. angle," (TVA), which was identified previously by Kostenbauder. This coupling between the *k-vector* and *time* has not received much attention, but, as we will show here, it is often present when other "better known" distortions are present. The presence of TVA indicates that the propagation direction of the pulse changes as the pulse proceeds in time, generating what we would like to point out might be called an "ultrafast lighthouse effect."

There is also a new spatio-temporal-coupling term, $\text{Im}\{P_{kt}\}$, which we refer to as the "angular temporal chirp" (ATC). Its effect is analogous to the one shown in figure 1, but the y-axis represents the k-vector instead of position.

4. Defining the widths in presence of spatio-temporal couplings

For a pulse that does not have spatio-temporal couplings, defining the widths (that is, the beam spot size, pulse width, bandwidth, and divergence angle) is straightforward. In the (x,t) domain, for example, one can find the beam spot size, in the root-mean-square definition, as:

$$\Delta x = \left[\frac{\int_{-\infty}^{\infty} x^2 I(x,t)dx - \left(\int_{-\infty}^{\infty} x I(x,t)dx \right)^2}{\int_{-\infty}^{\infty} I(x,t)dx} \right]^{1/2}$$

(26)

where *I(x,t)* is the pulse intensity in (x,t) domain. The second term in the numerator is simply the mean beam position and can be omitted when it is set to be zero. An analogous definition applies for the pulse width, bandwidth, and angular divergence.

If there is no coupling between t and x, then the intensity can be separated into x- and t-dependent parts; as a result, Eq. (26) yields the usual beam width definition with no t-dependence.

When there is coupling, however, the situation is more complex. The above definition could in principle yield a time-dependent Δx. For the Gaussians that we have been considering, however, this is not the case, and the beam size is independent of time. But in the presence of pulse-front tilt, the beam central position will depend on time (See Fig. 3-4), and the spot size at a given time will be less than the spot size integrated over all times. There are thus two types of width, one at a given time and another integrated over all time, as well as position. Since the intensity profile is usually measured with slow detectors, the intensity

profile $I(x,t)$ is usually integrated over time, as well. This will yield what could be called a "global" spot size (indicated by the subscript "G"), as opposed to the spot size at a given time, which we will call the "local" spot size, which is that given in Eq. (26) (and henceforth indicated by the subscript "L"). Thus:

$$\Delta x_L\left(t\right)=\left[\frac{\int_{-\infty}^{\infty}x^2 I(x,t)dx-\left(\int_{-\infty}^{\infty}xI(x,t)dx\right)^2}{\int_{-\infty}^{\infty}I(x,t)dx}\right]^{1/2} \tag{27}$$

$$\Delta x_G=\left[\frac{\int_{-\infty}^{\infty}\int_{-\infty}^{\infty}x^2 I(x,t)dxdt}{\int_{-\infty}^{\infty}\int_{-\infty}^{\infty}I(x,t)dxdt}\right]^{1/2} \tag{28}$$

where Δx_L and Δx_G are local and global beam widths, respectively. We have not subtracted off the mean in Eq. (28) as we have in Eq. (27) because it is always zero for the functions we are considering.

The idea of local and global widths apply to other parameters (pulse width, bandwidth and divergence angle) as well, in the same manner. We will, however, focus only on the width in the position, x, and time, t, since the others follow easily.

Taking the squared magnitude of Eq. (4) in Eq. (27) and in Eq. (28) we find:

$$\Delta x_L=\frac{1}{2}\left[-\frac{1}{\tilde{Q}_{xx}^{R}}\right]^{1/2} \tag{29}$$

$$\Delta x_G=\frac{1}{2}\left[-\frac{\tilde{Q}_{tt}^{R}}{\tilde{Q}_{xx}^{R}\tilde{Q}_{tt}^{R}+\tilde{Q}_{xt}^{R\,2}}\right]^{1/2} \tag{30}$$

Similarly, for the temporal widths, we obtain:

$$\Delta t_L=\frac{1}{2}\left[\frac{1}{\tilde{Q}_{tt}^{R}}\right]^{1/2} \tag{31}$$

$$\Delta t_G=\frac{1}{2}\left[\frac{\tilde{Q}_{xx}^{R}}{\tilde{Q}_{xx}^{R}\tilde{Q}_{tt}^{R}+\tilde{Q}_{xt}^{R\,2}}\right]^{1/2} \tag{32}$$

Equations (30) and (32) also reduce to the expected values when the cross term (PFT) is zero. Widths in other domains can be found simply by substituting $\tilde{Q}$ s with the corresponding coefficients in the particular domain. Thus the local widths are those that directly emerge from the diagonal components of the various matrices, while the global widths require knowledge of the off-diagonal components, that is, the spatio-temporal distortions.

5. Defining spatio-temporal couplings

We have identified the real parts of the cross terms in each domain as equivalent to the known spatio-temporal couplings. However, the dimensions of the various cross terms are unintuitive and do not correspond to easily understood definitions of spatio-temporal distortions. As a result, it is difficult to know whether a given amount of, say, spatial chirp is large or small. Thus, for experimental convenience and better intuition, normalization is helpful. As an example, we will work with $E(x,\omega)$ and express the spatial chirp in terms of the various coefficients of the R matrix.

To further complicate the issue, there are two definitions of spatial chirp, and each involves a partial derivative [2]. One is the "spatial dispersion (SPD)," $\partial x_0 / \partial \omega$, where x_0 is the mean beam position for a given frequency, ω. The other is the "frequency gradient (FRG)," $\partial \omega_0 / \partial x$, where ω_0 is the mean frequency for a given position, x.

Note from Eq. (12) that the term $R_{x\omega}$ has dimensions of $[x^{-1}\omega^{-1}]$, so it neither has the dimensions of $\partial x_0 / \partial \omega$, nor those of $\partial \omega_0 / \partial x$. To be able to express $R_{x\omega}$ in terms of the spatial dispersion or the frequency gradient, we must normalize it with respect to the beam width or frequency bandwidth. This is equivalent to expressing the pulse field (in the absence of imaginary components) in a form like:

$$E(x,\omega) \propto \exp\left[-\left(\frac{x - \frac{\partial x_0}{\partial \omega}\omega}{4\Delta x_L} \right)^2 - \frac{\omega^2}{4\Delta \omega_G^{\;2}} \right] \tag{33}$$

where $\partial x_0/\partial \omega$ is the spatial dispersion (SPD). We can rewrite our expression for the field in this form by simple rearrangement:

$$E(x,\omega) \propto \exp\left[R_{xx}^R x^2 + 2R_{x\omega}^R x\omega - R_{\omega\omega}^R \omega^2 \right]$$

$$= \exp\left[R_{xx}^R \left(x + \frac{R_{x\omega}^R}{R_{xx}^R}\omega \right)^2 - \left(\frac{R_{x\omega}^{R\;2}}{R_{xx}^R} + R_{\omega\omega}^R \right)\omega^2 \right] \tag{34}$$

where we have used a shortcut notation, superscript "R", for the real part of the parameter. We can now identify the quantities:

$$\Delta x_L = \frac{1}{2}\left[-\frac{1}{R_{xx}^R} \right] = \frac{w}{2} \tag{35}$$

is the spot size of each frequency component, or the local beam width. Also,

$$\frac{\partial x_0}{\partial \omega} = -\frac{R_{x\omega}^R}{R_{xx}^R} \tag{36}$$

is the spatial dispersion. And finally,

$$\Delta\omega_G = \frac{1}{2}\left(\frac{R_{xx}^R}{R_{x\omega}^{R\ 2} + R_{\omega\omega}^R R_{xx}^R}\right)^{1/2} \tag{37}$$

is the global bandwidth.

Alternatively, we can write the field in terms of the frequency gradient (FRG), represented here by $d\omega_0/dx$:

$$
\begin{aligned}
E(x,\omega) &= \exp\left[-\frac{x^2}{4\Delta x_G^2} - \left(\frac{\omega - \frac{\partial\omega_0}{\partial x}x}{4\Delta\omega_L}\right)^2\right] \\
&= \exp\left[\left(\frac{R_{x\omega}^{R\ 2}}{R_{\omega\omega}^R} + R_{xx}^R\right)x^2 - R_{\omega\omega}^R\left(\omega - \frac{R_{x\omega}^R}{R_{\omega\omega}^R}x\right)^2\right]
\end{aligned} \tag{38}
$$

where

$$\Delta x_G = \frac{1}{2}\left(-\frac{R_{\omega\omega}^R}{R_{x\omega}^{R\ 2} + R_{\omega\omega}^R R_{xx}^R}\right)^{1/2} \tag{39}$$

is the global beam width,

$$\frac{\partial\omega_0}{\partial x} = \frac{R_{x\omega}^R}{R_{\omega\omega}^R} \tag{40}$$

is the frequency gradient, and

$$\Delta\omega_L = \frac{1}{2}\left[\frac{1}{R_{\omega\omega}^R}\right]^{1/2} \tag{41}$$

is the local pulse bandwidth.

It is also easy to derive a relation between spatial dispersion and frequency gradient using Eqs. (36)-(40):

$$\frac{\partial\omega_0}{\partial x} = \frac{\dfrac{\partial x_0}{\partial\omega}}{\left(\dfrac{\partial x_0}{\partial\omega}\right)^2 + \dfrac{\Delta x_L^2}{\Delta\omega_G^2}} \tag{42}$$

which is identical to the relation found in [2].

It is also possible to define the spatial chirp as a dimensionless quantity, considered as a type of "correlation coefficient," by normalizing with respect to both beam width and bandwidth. The correlation coefficient (normalized) is defined as:

$$\rho_{x\omega} \equiv \frac{\iint x\omega I(x,\omega)dxd\omega}{\iint I(x,\omega)dxd\omega} \frac{1}{\Delta x_G \Delta\omega_G} \tag{43}$$

Then, in terms of the R coefficients, we find:

$$\rho_{x\omega} = \frac{R_{x\omega}^R}{\sqrt{-R_{xx}^R R_{\omega\omega}^R}} \tag{44}$$

Definitions of couplings in terms of correlation coefficients in all other domains can also be found simply by replacing R's in Eq. (44) by corresponding quantities. Defining the coupling in terms of these correlation coefficients has an advantage that the coefficient ρ always lies between 1 and -1. Therefore, this quantity can easily show whether the coupling is "large" or "small." It also does not vary as the beam propagates freely and potentially expands.

It is also possible to relate the global and local widths by the correlation coefficient. This results in:

$$\Delta x_L(\omega) = \Delta x_G \sqrt{1-\rho_{x\omega}^2} \tag{45}$$

$$\Delta\omega_L(x) = \Delta\omega_G \sqrt{1-\rho_{x\omega}^2} \tag{46}$$

Note that obtaining more intuitive, normalized quantities like SPD and FRG or dimensionless quantities from the cross terms only involves division by the beam width or the bandwidth or both (equivalents in the domain under investigation).

Thus, there are four distinct definitions of spatio-temporal couplings: 1) the cross term itself; 2,3) the cross term normalized by either the space/spatial-frequency or time/frequency width; and 4) the cross terms normalized by the product of the square roots of both the space/spatial-frequency and time/frequency width.

This same approach can be applied to the other domains, as well, yielding four definitions for each quantity. The second and third described above are analogous to the two definitions of spatial chirp as spatial dispersion or frequency gradient. For example, PFT can be viewed as the "arrival time (of maximum or mean intensity) vs. position" or "position (of maximum or mean intensity) vs. time."

6. Relations between the spatio-temporal couplings

To first order, there are four distinct real (amplitude) spatio-temporal couplings: PFT, SPC, AGD and TVA, and there are four imaginary (phase) spatio-temporal couplings: WFR, WFD, ASC and ATC. Obviously, they are not all independent; if one has all six (three real and three imaginary) coefficients in any single domain, say (x,t), then the field in all other domains can be calculated by taking Fourier transforms. Thus, for Gaussian pulse/beams, since four parameters are diagonal components that describe the pulse width, spot size, etc., there are only two independent spatio-temporal couplings. The other six can be computed from these two (and the relevant diagonal components, such as the pulse width, temporal chirp, spot size, and wave-front radius of curvature). In this section, we derive these relations explicitly.

First, we point out that we have actually already derived such general expressions in the forms of Eqs. (13), (16), and (22), as well as Eqs. (19) and (23). These equations yield all possible relations between the eight spatio-temporal distortions. These relations are

summarized in table 1 below. Each row of the table shows the cross terms in one domain and its equivalent representation in the others.

Table 1. Summary of the relations of spatio-temporal distortions in all four domains.

(x,t)	(x,ω)	(k,ω)	(k,t)
$\tilde{Q}_{xt}$	$\dfrac{i}{2}\dfrac{R_{x\omega}}{R_{\omega\omega}}$	$\dfrac{1}{4}\dfrac{S_{k\omega}}{S_{kk}S_{\omega\omega}+S_{k\omega}^2}$	$-\dfrac{i}{2}\dfrac{P_{kt}}{P_{kk}}$
$-\dfrac{i}{2}\dfrac{\tilde{Q}_{xt}}{\tilde{Q}_{tt}}$	$R_{x\omega}$	$-\dfrac{i}{2}\dfrac{S_{k\omega}}{S_{kk}}$	$\dfrac{1}{4}\dfrac{P_{kt}}{P_{kk}P_{tt}+P_{kt}^2}$
$\dfrac{1}{4}\dfrac{\tilde{Q}_{xt}}{\tilde{Q}_{xx}\tilde{Q}_{tt}+\tilde{Q}_{xt}^2}$	$\dfrac{i}{2}\dfrac{R_{x\omega}}{R_{xx}}$	$S_{k\omega}$	$-\dfrac{i}{2}\dfrac{P_{kt}}{P_{tt}}$
$\dfrac{i}{2}\dfrac{\tilde{Q}_{xt}}{\tilde{Q}_{xx}}$	$\dfrac{1}{4}\dfrac{R_{x\omega}}{R_{xx}R_{\omega\omega}+R_{x\omega}^2}$	$\dfrac{i}{2}\dfrac{S_{k\omega}}{S_{\omega\omega}}$	P_{kt}

While table 1 presents the complete listing of the relations between the first-order spatio-temporal couplings, these expressions are somewhat unintuitive, as they are expressed entirely in terms of the P, Q, R, and S matrices. Most of these equations, however, can easily be written in a more compact an intuitive manner.

We begin with the (x,t) domain. As indicated earlier, the real part of the cross term in the exponential of Eq. (4) denotes the PFT. Using table 1 and isolating the real part of $\tilde{Q}_{xt}$ in terms of the R's, we obtain:

$$\tilde{Q}_{xt}^R = \frac{1}{2|R_{\omega\omega}|^2}\left[-R_{\omega\omega}^R R_{x\omega}^I + R_{\omega\omega}^I R_{x\omega}^R\right] \qquad (47)$$

Again, we have used a compact notation of superscripts R and I to indicate the real and imaginary parts respectively. By using the normalization procedure we described earlier, we can write Eq. (47) in a much more intuitive form with dimensionless quantities:

$$\text{PFT} = - 2\,\text{WFD} + 2\,\text{FCH} \times \text{FRG} \qquad (48)$$

Where, PFT is normalized by TPW. We can also derive the relation involving pulse-front tilt, angular dispersion, spatial chirp, and temporal chirp that we mentioned earlier. If the beam is well collimated, the R_{xx} term can be assumed to be real (the imaginary part approaches zero when radius of curvature is very large). Then, using table 1, the real part of $S_{k\omega}$ (AGD) will be proportional to the imaginary part of $R_{x\omega}$ (WFD). Therefore, in the well-collimated-beam approximation, we can conclude that $R_{x\omega}^I$ is proportional to AGD. Recalling that $R_{\omega\omega}^I$ is the FCH and $R_{x\omega}^R$ is the SPC, we can translate Eq. (47) to words: "PFT is generated by AGD and simultaneous SPC and TPC", in perfect agreement with what was shown in [11]. If we express PFT in its form normalized only by the pulse width (and hence not dimensionless, but in units of [time/position]), we can write Eq. (47) as:

$$\text{PFT} = \text{AGD} + 2\,\text{FCH} \times \text{FRG} \qquad (49)$$

While Eq. (49) is valid in well collimated beam assumption, Eq. (47) is general and holds for diverging beams also. Therefore, it yields the change in PFT due to beam divergence as worked out in [21, 22].

Analogous forms of Eq. (48) can also be written for other domains. Skipping the details, we can list some of the relations as follows:

$$SPD = 2\,ASC - 2\,AGD \times APC \qquad (50)$$

Where, AGD is normalized by ADV. If the FCH is zero, then the ASC term will be proportional to TVA. In this case, this equation has a physical meaning of "SPD is generated by TVA and simultaneous AGD and APC". We should mention parenthetically that, while the assumption of well-collimated beams is reasonable for many practical situations, assuming zero FCH is not that practical, as ultrashort light pulses usually have some FCH resulting from propagation through dispersive optics. Therefore, for practical reasons, the full form of Eq. (50) is more useful.

Next, we can write:

$$AGD = -\,2\,ATC + 2\,TVA \times TCH \qquad (51)$$

Where, AGD is normalized by BDV and TVA is normalized by TPW. In the well-collimated beam approximation, ATC can be seen to be proportional to PFT. Then, Eq. (51) can be pronounced as "AGD is generated by PFT and simultaneous TVA and TCH".

Lastly:

$$TVA = -\,2\,WFR + 2\,PFT \times WFC \qquad (52)$$

Where, TVA is normalized by ADV and PFT is normalized by BSS. If the temporal chirp is zero, then the WFC term will be proportional to SPC. In this case, this equation has the physical meaning of "TVA is generated by SPC and simultaneous PFT and WFC." As noted earlier, the zero temporal chirp assumption is generally not very practical, so the full form of Eq. (52) is recommended for practical use.

7. Constructing the electric field in different domains

Having derived the expressions that relate spatio-temporal couplings, we can now construct the pulse field with the knowledge of the pulse parameters. We will start in (x,t) domain, and then the other domains will follow easily from (inverse) Fourier transforms.

From Eq.(4), it is clear that, to be able to explicitly write the pulse electric field in this form, one needs only six independent parameters (real and imaginary parts of the Q coefficients). Namely, one needs BSS, WFC, TPW, TCH, PFT and WFR. The spatial and temporal parameters, as well as PFT can be measured with well established pulse characterized methods [3, 23-25] (see next section for details on this). While, the full field can be determined by additionally determining WFR, in general, it is experimentally difficult to directly measure this quantity. In general, it is experimentally easier to measure intensity couplings, than phase couplings. Therefore it would be very useful if we could express WFR (or other phase couplings) in terms of the intensity couplings. Using the relations in table 1, and after some manipulations, we derive:

$$\widetilde{Q}_{xt} = \frac{i}{2}\,FRG + \widetilde{Q}_{tt}\,PFT \qquad (53)$$

which can also be written as:

$$\text{WFR} = \frac{\text{FRG}}{2} + \text{TCH} \times \text{PFT} \tag{54}$$

In this expression, the PFT is normalized only by the pulse width. Eq. (54) is very useful, as it shows that the phase coupling, WFR, can be expressed in terms of intensity couplings and easier-to-measure parameters. Therefore, in addition to the pulse spatial and temporal parameters and PFT, mentioned above, if one knows the FRG as well, then the complete Gaussian pulse/beam field is known.

To summarize this section, there are only six independent parameters required to find the full Gaussian spatio-temporal pulse electric field in all of the four domains. For example, the knowledge of BSS, WFC, TPW, TCH, PFT and SPC is sufficient to determine the full pulse electric field. All other spatio-temporal couplings can also be found from these six parameters. This is significant because single-shot FROG and GRENOUILLE methods, for example, allow the measurement of the SPC and PFT, as well as TPW and TCH. Therefore, an additional (relatively straightforward) measurement of BSS and WFC fully determines the spatio-temporal pulse-field in all four domains.

This set of parameters assumes, of course, operation in the (x,t) domain. We could alternatively operate in another domain, in which case we would need another set of six parameters. We can also derive expressions like Eq. (54) that relate the phase couplings to the intensity couplings. These expressions are:

$$\text{WFD} = -\frac{\text{AGD}}{2} + \text{SPD} \times \text{WFC} \tag{55}$$

$$\text{ASC} = -\frac{\text{TVA}}{2} + \text{AGD} \times \text{FCH} \tag{56}$$

$$\text{ATC} = \frac{\text{PFT}}{2} + \text{TVA} \times \text{APC} \tag{57}$$

In the figures below, we illustrate the ideas of this section. Starting only with the six parameters mentioned above, we constructed the pulse electric filed in all domains. Figure 3 and 4 show the intensity profiles of such a pulse in the various domains. Note that the intensity traces are tilted in each of the four domains, indicating the presence of all four spatio-temporal couplings. Tables 2 and 3 show the spatio-temporal couplings in each domain expressed in terms of dimensionless correlation coefficients. Note that the correlation coefficients intuitively describe both the magnitude and sign of the couplings.

Some of the input parameters for the pulse shown in figure 3 are as follows: Center wavelength = 800 nm, Δx_G = 2.56 mm. Δt_G = 82.1 fs, TCH = 6.2×10^{-4} fs^{-2}. And coupling values are PFT = 7 fs/mm. SPD = 3.4 mm.fs/rad. These values of PFT and SPD correspond to the following experimental situation: an anti-parallel prism pair, each prism made of fused silica with apex angles of 69 degree. The prisms are separated by 310 mm. The first prism is used at Brewster's angle and the second one is tilted from Brewster's angle by 1.5 degrees.
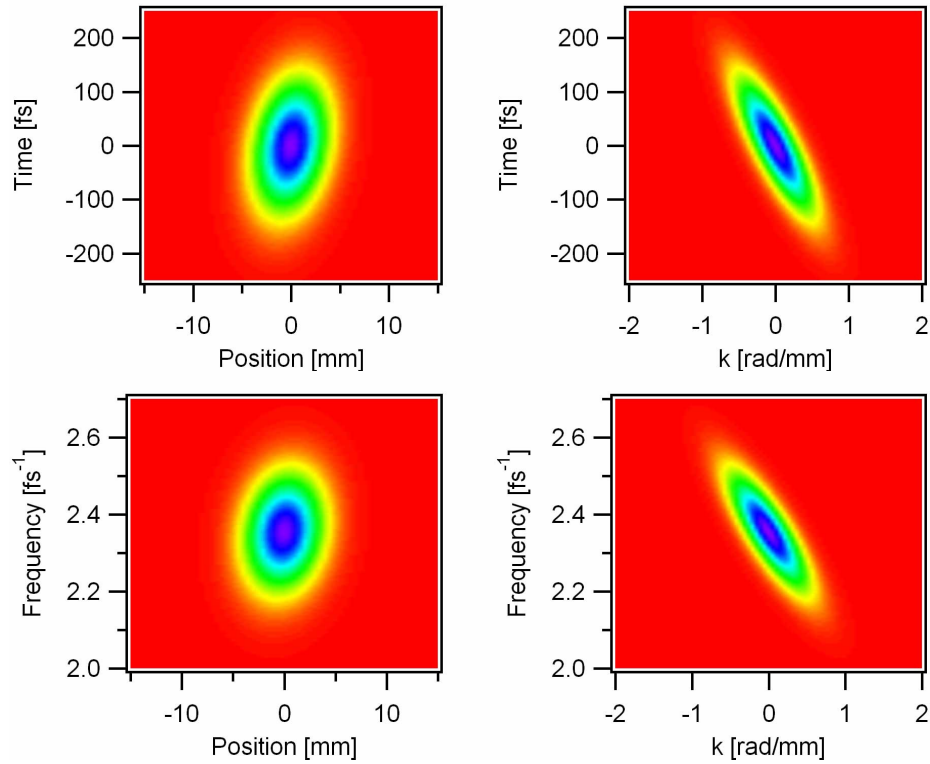
Fig. 3. Intensity profile of a pulse expressed in the four different domains. This pulse simultaneously has all four spatio-temporal amplitude couplings: PFT, SPC, AGD and TVA, as can be seen from the tilted images.

Table 2 The correlation coefficients of the pulse field shown in Figure 3.

Coupling	ρ_{xt}	ρ_{kt}	$\rho_{x\omega}$	$\rho_{k\omega}$
value	0.22	−0.81	0.14	−0.82

The same set of input parameters for the case of the pulse shown in figure 4 are as follows: Center wavelength = 800 nm, Δx_G = 2.95 mm. Δt_G = 94.5 fs, TCH = -6.2x10^{-4} fs^{-2}. And coupling values are PFT = 17 fs/mm. SPD = 13.3 mm.fs/rad. These values of PFT and SPD correspond to the following experimental situation: an anti-parallel prism pair, each prism made of fused silica with apex angle of 69 degree. The prisms are separated by 1130 mm. The first prism is used at Brewster's angle and the second one is tilted from Brewster's angle by 0.05 degrees.

From the traces in Figs. 3 and 4, the couplings in other normalizations can also be calculated. The slope of the trace in the (x,t) domain is the PFT; in the (x,ω) domain it is SPC; in (k,ω) it is AGD; and in (k,t) it is TVA. As indicated in section 5, to find these slopes, there are two distinct approaches, and each gives a proper description of the coupling under investigation. For example, in the (x,ω) trace, if the slope is found by finding the center position at each frequency, then the measured parameter is the SPD. When the slope is found by finding the center frequency at each position, then the measured parameter is FRG.
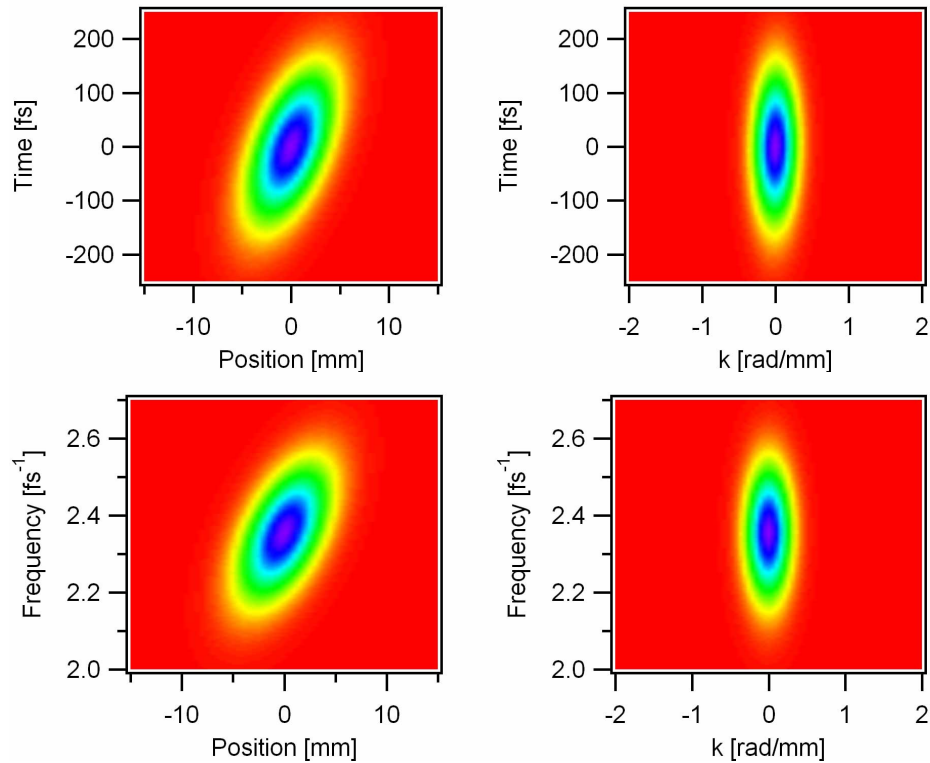
Fig. 4. Intensity profile of a pulse expressed in the four different domains. This pulse has significant PFT and SPC but very small AGD and TVA, as can be seen from the tilt of the traces.

Table 3. The correlation coefficients of the pulse field shown in Fig. 4.

Coupling	ρ_{xt}	ρ_{kt}	$\rho_{x\omega}$	$\rho_{k\omega}$
value	0.53	0.04	0.53	0.01

8. Approach for the experiments

In this section, we would like to describe an experimental approach to determine the spatio-temporal pulse field, using the ideas we described in this paper. Although there are numerous possible ways, we describe a sample method that we think is one of the most straightforward.

As noted earlier, there are only six independent parameters required to completely determine the pulse in all domains. In the (x,t) domain, these parameters are: BSS, WFC, TPW, TCH, PFT and SPC.

The temporal width and chirp can be measured using some convenient ultrashort-pulse measurement techniques available like FROG or GRENOUILLE [24, 25].

To measure PFT, one can use GRENOUILLE or other techniques [4, 5, 21, 26]. To measure SPC with high sensitivity, one can use an imaging spectrometer [2].

Finally, to measure the spatial parameters, one can simply use a CCD. This measurement, however, inherently yields the *global* beam width as the slow CCD integrates over time. Then, using Eq. (30), the Q parameter (real part only) can be determined. While the imaginary part is very small, and hence negligible, for well collimated beams, a wave-front measurement technique can be applied, if needed [27].

These measurements completely determine the set of numbers that is needed to complete determine a Gaussian ultrashort pulse, and all of the spatio-temporal couplings in all four of the domains.

9. Conclusion

In conclusion, we demonstrated a simple approach in determining and describing the spatio-temporal couplings/distortions in ultrashort pulses. Our approach completely determines the explicit relations between all the various spatio-temporal couplings. It can also be generalized to arbitrary profiles by using computational analysis instead of the analytical approach described here. We hope that our calculations and definitions will provide a useful tool for ultrafast-optics researchers to better understand the distortions that commonly occur (intentionally or not) in ultrashort pulses.